SO(4) gauged O(5) Skyrmion on $\mathbf{R}^4$

Francisco Navarro-Lérida[*]
Departamento de Física Teórica and IPARCOS, Ciencias Físicas, Universidad Complutense de Madrid, E-28040 Madrid, Spain

D. H. Tchrakian[†]
School of Theoretical Physics, Dublin Institute for Advanced Studies, Burlington Road, Dublin 4, Ireland and Department of Computer Science, Maynooth University, Maynooth, Ireland

(Received 2 September 2025; accepted 16 October 2025; published 7 November 2025)

We have studied an $SO(4)$ gauged $O(5)$ Skyrmion on $\mathbf{R}^4$, which can be seen as a static soliton in $4+1$ dimensions. This is a sequel of the known $SO(D)$ gauged $O(D+1)$ Skyrmions on $\mathbf{R}^D$ in $D=2$ and in $D=3$, which are likewise localized to an absolute scale and topologically stable, their energies being bounded below by the winding number. In the absence of an analytic proof of existence, some such solutions are constructed numerically. Two families of solutions are found, of which only one possesses a gauge decoupling limit. The curvatures of both of these solutions decay as r^{-3}, a property they share with the Yang-Mills instantons on $\mathbf{R}^4$.

DOI: 10.1103/pg5m-7cl3

I. INTRODUCTION AND PRELIMINARIES

Since the work of Schroers [1] on the $SO(2)$ gauged $O(3)$ Skyrmions on $\mathbf{R}^2$, there has been considerable interest in carrying out the corresponding analysis on the $SO(3)$ gauged $O(4)$ Skyrmions [2] on $\mathbf{R}^3$ [4–8]. It is our aim here to extend this analysis to the next step of constructing an $SO(4)$ gauged $O(5)$ Skyrmion on $\mathbf{R}^4$—namely, to the $D=4$ case, which points out the extension to arbitrary D.

With the exception of the solutions in $D=2$ [1] where analytic proofs of existence for solutions subject to no symmetries are given in Refs. [9,10] and in Ref. [11], solutions in $D=3$ [4,5] are studied only subject to radial symmetry where the resulting ordinary differential equations (ODEs) are solved numerically. Here too, we restrict our study to the radially symmetric case and construct the solutions numerically. In the absence of a compelling physical reason to consider less symmetric solutions—e.g., axial symmetry—and given the complexity of the system, this is a reasonable approach.

The solutions constructed here have finite energy and are topologically stable, stabilized by the Skyrme-Chern-Pontryagin (SCP) charges defined in Ref. [12] for $D \leq 5$. These charge densities enable the construction of the models in $D=2$, 3 and here in $D=4$, by exploiting Bogomol'nyi-like inequalities [13].

To be self-contained and to fix the notation, we give a brief description of the SCP topological charge used here. In D dimensions, the definitions of the winding number density of ϕ^A, and its gauge covariantized version $\varrho_G^{(D)}$ for gauge group $SO(D)$, are

$$\varrho_0^{(D)} = \varepsilon_{i_1 i_2 .. i_D} \varepsilon^{A_1 A_2 .. A_D A_{D+1}} \times \partial_{i_1} \phi^{A_1} \partial_{i_2} \phi^{A_2} \ldots \partial_{i_D} \phi^{A_D} \phi^{A_{D+1}}, \tag{1}$$

$$\varrho_G^{(D)} = \varepsilon_{i_1 i_2 .. i_D} \varepsilon^{A_1 A_2 .. A_D A_{D+1}} \times D_{i_1} \phi^{A_1} D_{i_2} \phi^{A_2} \ldots D_{i_D} \phi^{A_D} \phi^{A_{D+1}}, \tag{2}$$

where the $SO(D)$ covariant derivatives $D_i\phi^a$ and $D_i\phi^{D+1}$ are defined as

$$D_i\phi^a = \partial_i\phi^a + A_i^{ab}\phi^b \quad a = 1, 2, \ldots, D, \tag{3}$$

$$D_i\phi^{D+1} = \partial_i\phi^{D+1}, \tag{4}$$

with A_i^{ab} being the $SO(D)$ gauge connection. Summation over repeated indices is assumed.

[*]Contact author: fnavarro@ucm.es
[†]Contact author: tigran@stp.dias.ie

Published by the American Physical Society under the terms of the Creative Commons Attribution 4.0 International license. Further distribution of this work must maintain attribution to the author(s) and the published article's title, journal citation, and DOI. Funded by SCOAP³.

The $SO(D)$ gauge curvature is defined by $F_{ij}^{ab}\phi^b = D_{[i}D_{j]}\phi^a$, which explicitly reads

$$F_{ij}^{ab} = \partial_{[i}A_{j]}^{ab} + (A_{[i}A_{j]})^{ab}, \tag{5}$$

where

$$(A_iA_j)^{ab} = A_i^{ac}A_j^{cb} \quad a,b = 1,2,\ldots,D. \tag{6}$$

The method of construction of Skyrme-Chern-Pontryagin densities, which are both *gauge invariant* and *total divergence*, is given in Ref. [12].

The prescription for constructing the SCP densities hinges on evaluating the difference

$$\varrho_G^{(D)} - \varrho_0^{(D)}$$

and entails casting it in the form

$$\varrho_G^{(D)} - \varrho_0^{(D)} = \partial_i\Omega_i^{(D)}[A,\phi] - W^{(D)}[F,D\phi], \tag{7}$$

in which $W^{(D)}[F,D\phi]$ is *gauge invariant* and the vector-valued density $\Omega_i^{(D)}[A,\phi]$ is *gauge variant*.

From Eq. (7), one can define the density:

$$\varrho \overset{\text{def.}}{=} \varrho_G^{(D)} + W^{(D)}[F,D\phi] \tag{8}$$

$$\overset{\text{def.}}{=} \varrho_0^{(D)} + \partial_i\Omega_i^{(D)}[A,\phi], \tag{9}$$

which is both *gauge invariant* [Eq. (8)] and *total divergence*, [Eq. (9)], since $\varrho_0^{(D)}$ is essentially a total divergence.

The definition (8) can be exploited for constructing Bogomol'nyi-like lower bounds, while the volume integral of Eq. (9) gives the topological charge, which equals the *winding number*, as the surface integral of $\Omega_i^{(D)}$ vanishes.

In Sec. II, the model under study is derived. In Sec. III, spherical symmetry is imposed, the resulting one-dimensional system is presented, and the boundary values are fixed. Section IV is devoted to the numerical construction of the solutions, and a summary and discussion is presented in Sec. V.

II. THE $SO(4)$ GAUGED $O(5)$ SKYRME MODEL ON $\mathbb{R}^4$

To emphasize the restriction to $\mathbb{R}^4$, we convert all D-dimensional Latin indices, $i,j,\ldots$, in the previous section to four-dimensional Greek indices, $\mu,\nu,\ldots$, here.

The quantities $W^{(D)}$ and $\Omega_\sigma^{(D)}$ appearing in Eqs. (8) and (9) for $D=4$ are [12]

$$W^{(4)} = \frac{3!}{4}\varepsilon_{\mu\nu\rho\sigma}\varepsilon^{fgab}\phi^5\left[\frac{1}{6}(\phi^5)^2F_{\mu\nu}^{fg}F_{\rho\sigma}^{ab} + F_{\mu\nu}^{fg}\phi_{\rho\sigma}^{ab}\right], \tag{10}$$

$$\Omega_\sigma^{(4)} = \phi^5\left(\partial_\mu\Omega_{\mu\sigma} + \frac{1}{2}\varepsilon_{\mu\nu\rho\sigma}\varepsilon^{fgab}\left[F_{\mu\nu}^{fg}\phi^aD_\rho\phi^b + \frac{1}{2}\left(1-\frac{1}{3}(\phi^5)^2\right)\Xi_{\mu\nu\rho}^{fgab}\right]\right), \tag{11}$$

where $\phi_{\mu\nu}^{ab}$ in Eq. (10) denotes

$$\phi_{\mu\nu}^{ab} = D_{[\mu}\phi^aD_{\nu]}\phi^b, \qquad [\mu\nu] = -[\nu\mu], \tag{12}$$

and in Eq. (11),

$$\Omega_{\mu\sigma} = \varepsilon_{\mu\nu\rho\sigma}\varepsilon^{fgab}A_\rho^{fg}\phi^a\left(\partial_\nu\phi^b + \frac{1}{2}A_\nu\phi^b\right), \tag{13}$$

$$\Xi_{\mu\nu\rho}^{fgab} = A_\rho^{ab}\left[\partial_\mu A_\nu^{fg} + \frac{2}{3}(A_\mu A_\nu)^{fg}\right]. \tag{14}$$

$W^{(4)}$ defined by Eq. (10) is the density in Eq. (8) for $D=4$, which can be used to state Bogomol'nyi-like inequalities leading to the energy-density functional that describes the soliton—namely, Eq. (8) for $D=4$:

$$\varrho^{(4)} = \varrho_G^{(4)} + W^{(4)}. \tag{15}$$

However, Eq. (10) is not the most general such density, as indeed, in all even dimensions, the Chern-Pontryagin (CP) density, which is itself both *gauge invariant* and *total divergence*, can be added to/subtracted from the definitions of (8) or (9) without changing these *properties* in either case. This has been exploited in the $D=2$ case in Refs. [14,15]. In particular, in Appendix A of Ref. [14], it is explained why the inclusion of the CP density is necessary for supporting finite-energy solutions.

In the present case, this is the second CP density

$$-\frac{1}{4}\varepsilon_{\mu\nu\rho\sigma}\varepsilon^{fgab}F_{\mu\nu}^{fg}F_{\rho\sigma}^{ab} = \varepsilon_{\mu\nu\rho\sigma}\varepsilon^{fgab}\partial_\sigma\left\{A_\rho^{fg}\left[\partial_\mu A_\nu^{ab} + \frac{2}{3}(A_\mu A_\nu)^{ab}\right]\right\}, \tag{16}$$

with the left-hand side (with the negative sign) being added to Eq. (8) and the right-hand side added to Eq. (9).

Adding the lhs of (16) to Eq. (10), and its rhs to Eq. (11), we have the alternative definition of the SCP density in $D=4$:

$$\tilde{W}^{(4)} = \frac{3!}{4}\varepsilon_{\mu\nu\rho\sigma}\varepsilon^{fgab} \times \left\{\frac{1}{6}[(\phi^5)^3-1]F_{\mu\nu}^{fg}F_{\rho\sigma}^{ab} + \phi^5F_{\mu\nu}^{fg}\phi_{\rho\sigma}^{ab}\right\}, \tag{17}$$

$$\tilde{\Omega}^{(4)}_{\sigma} = \phi^5\Big(\partial_\mu\Omega_{\mu\sigma} + \frac{1}{2}\varepsilon_{\mu\nu\rho\sigma}\varepsilon^{fgab}\Big[F^{fg}_{\mu\nu}\phi^a D_\rho\phi^b + \frac{1}{2}\Big(3-\frac{1}{3}(\phi^5)^2\Big)\Xi^{fgab}_{\mu\nu\rho}\Big]\Big), \tag{18}$$

leading to the definition of the "improved" topological charge density:

$$\tilde{\varrho}^{(4)} = \varrho^{(4)}_G + \tilde{W}^{(4)}. \tag{19}$$

Before proceeding to state the Bogomol'nyi-like inequalities in the next subsection, the choice of topological charge density—either (15) or (19)—must be made. Our choice here is the "improved" density in Eq. (19) rather than (15), because the first term in Eq. (17),

$$[(\phi^5)^3 - 1]F^{fg}_{\mu\nu}F^{ab}_{\rho\sigma}, \tag{20}$$

leads to the definition of a (chiral) self-interaction potential in the same way as in the $D = 2$ case [1,14,15]. The difference is that in the $D = 2$ case, it is necessary to incorporate the self-interaction potential in the topological charge density for it to lead to a finite energy lower bound, while in $D = 4$ this is not necessary. We have nonetheless opted here for the "improved" density in Eq. (19), as the presence of the potential facilitates the numerical construction, which is the main means to prove the existence here.

A. Lower bounds and choice of model

To reproduce the first term in $\tilde{W}^{(4)}$ defined by Eq. (17), appearing in Eq. (19), consider the inequality

$$|(\tau_1\eta^{-2}F(4) - \tau\eta^2[(\phi^5)^3 - 1])|^2 \geq 0, \quad [\eta] = L^{-1}, \tag{21}$$

in which $F(4)$ is defined as

$$F(4) \overset{\text{def.}}{=} \varepsilon_{\mu\nu\rho\sigma}\varepsilon^{abcd}F^{ab}_{\mu\nu}F^{cd}_{\rho\sigma}. \tag{22}$$

Defining further the "potential"

$$V[\phi^5] \overset{\text{def.}}{=} [(\phi^5)^3 - 1]^2, \tag{23}$$

the inequality (21) reads

$$(\tau_1^2\eta^{-4}F(4)^2 + \tau^2\eta^4 V[\phi^5]) \geq 2\tau\tau_1\varepsilon_{\mu\nu\rho\sigma}\varepsilon^{abcd}[(\phi^5)^3 - 1]F^{ab}_{\mu\nu}F^{cd}_{\rho\sigma}, \tag{24}$$

the rhs of which reproduces the first term in Eq. (19).

To reproduce the second term in $\tilde{W}^{(4)}$, consider the inequality

$$\Big|\Big(\tau_2\phi^5F^{fg}_{\mu\nu} - \frac{1}{2^2}\tau_3\varepsilon_{\mu\nu\rho\sigma}\varepsilon^{fgab}\phi^{ab}_{\rho\sigma}\Big)\Big|^2 \geq 0, \tag{25}$$

which leads to

$$\tau_2^2(\phi^5)^2|F^{fg}_{\mu\nu}|^2 + \tau_3^2|\phi^{fg}_{\mu\nu}|^2 \geq \frac{1}{2}\tau_2\tau_3\varepsilon_{\mu\nu\rho\sigma}\varepsilon^{fgab}\phi^5F^{fg}_{\mu\nu}\phi^{ab}_{\rho\sigma}. \tag{26}$$

Adding $\frac{1}{8}$ times Eq. (24) to 3 times Eq. (26), we have the inequality

$$\frac{1}{8}(\tau_1^2\eta^{-4}F(4)^2 + \tau^2\eta^4V[\phi^5]) + 3\tau_2^2(\phi^5)^2|F^{fg}_{\mu\nu}|^2 + 3\tau_3^2|\phi^{fg}_{\mu\nu}|^2 \geq \tilde{W}^{(4)}, \tag{27}$$

provided that

$$\tau\tau_1 = 1 \quad \text{and} \quad \tau_2\tau_3 = 1, \tag{28}$$

where $\tilde{W}^{(4)}$ is the density appearing in the definition (19) of the topological charge density.

To complete the rhs of the topological charge density (19), we need to add $\varrho^{(4)}_G$. This can be achieved by invoking the inequality [16]

$$|(\tau_4\kappa^{-1}\phi^A_\mu - \tau_5\kappa\tilde{\phi}^A_\mu)|^2 \geq 0, \tag{29}$$

in which the constant κ has the dimension of length, $[\kappa] = L$, and the quantity $\tilde{\phi}^A_\mu$ is defined as

$$\tilde{\phi}^A_\mu \overset{\text{def.}}{=} \varepsilon_{\mu\nu\rho\sigma}\varepsilon^{ABCDE}\phi^B_\nu\phi^C_\rho\phi^D_\sigma\phi^E. \tag{30}$$

The inequality in Eq. (29) now leads to

$$\frac{1}{2}(\tau_4^2\kappa^{-2}|\phi^A_\mu|^2 + \tau_5^2\kappa^2|\tilde{\phi}^A_\mu|^2) \geq \varrho^{(4)}_G, \tag{31}$$

provided that

$$\tau_4\tau_5 = 1. \tag{32}$$

Finally, adding Eq. (27) to Eq. (31), we end up with the energy density

$$\tilde{\mathcal{E}} = \frac{1}{8}(\tau_1^2\eta^{-4}F(4)^2 + \tau^2\eta^4V[\phi^5]) + 3\tau_2^2(\phi^5)^2|F^{fg}_{\mu\nu}|^2 + 3\tau_3^2|\phi^{fg}_{\mu\nu}|^2 + \frac{1}{2}(\tau_4^2\kappa^{-2}|\phi^A_\mu|^2 + \tau_5^2\kappa^2|\tilde{\phi}^A_\mu|^2), \tag{33}$$

which is bounded from below by the topological charge density (19):

$$\tilde{\varrho}^{(4)} = \varrho_G^{(4)} + \tilde{W}^{(4)}. \tag{34}$$

It may be worth remarking that saturating the Bogomol'nyi-like lower bounds stated by the inequalities in Eqs. (21), (25), and (29) results in the trivial solution, since the ensuing equations are overdetermined.

B. Scaling

The energy density [Eq. (33)] contains eight parameters $\{\tau, \tau_1, \ldots, \tau_5, \eta, \kappa\}$, subject to three constraints given by Eqs. (28) and (32). However, after rescaling properly, the effective number of free parameters may be reduced to only two parameters. In order to show this, we introduce the following dimensionless barred quantities, together with the dimensionless parameters α and β:

$$x^\mu = \tau_5\kappa\bar{x}^\mu, \qquad \eta = \beta^{1/4}\tau^{-1/2}(\tau_5\kappa)^{-1}, \tag{35}$$

$$\alpha = \tau_3^2, \qquad A_\mu^{fg} = (\tau_5\kappa)^{-1}\bar{A}_\mu^{fg}, \tag{36}$$

$$F_{\mu\nu}^{fg} = (\tau_5\kappa)^{-2}\bar{F}_{\mu\nu}^{fg}, \qquad F(4) = (\tau_5\kappa)^{-4}\bar{F}(4), \tag{37}$$

$$\phi^A = \bar{\phi}^A, \qquad \phi_\mu^A = (\tau_5\kappa)^{-1}\bar{\phi}_\mu^A, \tag{38}$$

$$\phi_{\mu\nu}^{AB} = (\tau_5\kappa)^{-2}\bar{\phi}_{\mu\nu}^{AB}, \qquad \tilde{\phi}_\mu^A = (\tau_5\kappa)^{-3}\bar{\tilde{\phi}}_\mu^A. \tag{39}$$

When this rescaling is introduced in Eq. (33), we get

$$\tilde{\mathcal{E}} = (\tau_5\kappa)^{-4}\left\{\frac{1}{8}(\beta^{-1}\bar{F}(4)^2 + \beta V[\bar{\phi}^5]) + 3\alpha^{-1}(\bar{\phi}^5)^2|\bar{F}_{\mu\nu}^{fg}|^2 + 3\alpha|\bar{\phi}_{\mu\nu}^{fg}|^2 + \frac{1}{2}(|\bar{\phi}_\mu^A|^2 + |\bar{\tilde{\phi}}_\mu^A|^2)\right\}, \tag{40}$$

so, choosing units such that $\tau_5\kappa = 1$, we obtain the energy density we will use for numerics:

$$\tilde{\mathcal{E}} = \frac{1}{8}(\beta^{-1}F(4)^2 + \beta V[\phi^5]) + 3\alpha^{-1}(\phi^5)^2|F_{\mu\nu}^{fg}|^2 + 3\alpha|\phi_{\mu\nu}^{fg}|^2 + \frac{1}{2}(|\phi_\mu^A|^2 + |\tilde{\phi}_\mu^A|^2), \tag{41}$$

where we have suppressed all upper bars for economy.

III. IMPOSITION OF RADIAL SYMMETRY

Subject to spherical symmetry, the $SO(4)$ gauge connection on $\mathbf{R}^4$ is parametrized by a radial function $w(r)$ as by the ansatz

$$A_\mu^{ab} = -\left(\frac{1 \pm w(r)}{r}\right)\delta_\mu^{[a}\hat{x}^{b]}; \quad \hat{x}^a = \frac{x^a}{r} \quad a = 1,2,3,4. \tag{42}$$

Subject to Eq. (42), the $|F_{\mu\nu}^{ab}|^2$ term is

$$|F_{\mu\nu}^{ab}|^2 = \frac{12}{r^2}\left[(w')^2 + \frac{1}{r^2}(1-w^2)\right], \tag{43}$$

and the square of the $F(4)$ term in Eq. (22) is

$$F(4)^2 = (4\times 4!)^2\frac{(w')^2}{r^6}(1-w^2)^2. \tag{44}$$

Subject to this symmetry, the real-valued (dimensionless) Skyrme scalar $\phi^A = (\phi^a, \phi^5)$ is parametrized by the dimensionless radial function $f(r)$ according to

$$\phi^a = \sin f(r)\widehat{x^a}, \tag{45}$$

$$\phi^5 = \cos f(r). \tag{46}$$

Denoting the $SO(4)$ covariant derivatives as

$$\phi_\mu^a \overset{\text{def.}}{=} D_\mu\phi^a \quad \text{and} \quad \phi_\mu^5 \overset{\text{def.}}{=} D_\mu\phi^5, \tag{47}$$

subject to the ansatz (42) and Eqs. (45) and (46), Eq. (47) becomes

$$\phi_\mu^a = \left[\left(f'\cos f \pm \frac{w\,\sin f}{r}\right)\hat{x}_\mu\hat{x}^a \mp \frac{w\,\sin f}{r}\delta_i^a\right], \tag{48}$$

$$\phi_\mu^5 = -(f'\sin f)\hat{x}_\mu, \tag{49}$$

resulting in the quadratic Skyrme kinetic term

$$|\phi_\mu^A|^2 = (f')^2 + \frac{3}{r^2}w^2\sin^2 f. \tag{50}$$

The quartic [17] Skyrme kinetic term $|\phi_\mu^{ab}|^2$ in the energy (33) is readily calculated to be

$$|\phi_{\mu\nu}^{ab}|^2 = 2\times 3!\left(\frac{w\,\sin f}{r}\right)^2\left[(f'\cos f)^2 + \left(\frac{w\,\sin f}{r}\right)^2\right]. \tag{51}$$

The sextic term in the energy density (33) is $|\tilde{\phi}_\mu^A|^2$, with $\tilde{\phi}_\mu^A$ defined by Eq. (30), which yields

$$|\tilde{\phi}^A|^2 = |\phi_{\mu\nu\lambda}^{ABC}|^2 = (3!)^2\left(\frac{w\,\sin f}{r}\right)^4 \times\left[3(f')^2 + \left(\frac{w\,\sin f}{r}\right)^2\right]. \tag{52}$$

Substituting Eqs. (42), (45), and (46) into the "energy" density functional (41) and multiplying the latter by r^3, coming from the volume element, we have the one-dimensional "energy" density. The resulting one-dimensional ODEs are not displayed here, since they are quite cumbersome.

A. Boundary conditions and expansions

Substituting the spherical ansatz [Eq. (42)] and Eqs. (45) and (46) into the field equations derived variationally from Eq. (41) subject to the constraint $|\phi^A|^2 = 1$, we obtain a system of two second-order equations for $f(r)$ and $w(r)$. Solutions to that system that have finite energy must satisfy

$$f(0) = \pi, \qquad w(0) = 1, \tag{53}$$

$$\lim_{r\to\infty} f(r) = 0, \qquad \lim_{r\to\infty} w(r) \equiv w_\infty = \pm 1. \tag{54}$$

Note that the presence of the $|F^{ab}_{\mu\nu}|^2$ term prevents the existence of monopole-type solutions with $\lim_{r\to\infty} w(r) = 0$, since that would lead to infinite-energy configurations, as seen clearly from Eq. (43).

Under Eqs. (53) and (54), the expansion of the solutions at the origin reads

$$f(r) = \pi + f_1 r + O(r^3), \qquad w(r) = 1 + w_2 r^2 + O(r^4), \tag{55}$$

while their asymptotic expansion results in

$$f(r) = \frac{\hat{f}_3}{r^3} + O\left(\frac{1}{r^5}\right), \quad w(r) = \pm 1 + \frac{\hat{w}_2}{r^2} + O\left(\frac{1}{r^4}\right), \tag{56}$$

where $f_1, w_2, \hat{f}_3, \hat{w}_2$ are constants determined numerically.

IV. RESULTS

We have solved the field equations derived from (41), subject to the spherical ansatz, by using the software package COLSYS, which employs a collocation method for boundary-value ordinary differential equations and a damped Newton method of quasilinearization [18]. The only free parameters in this model are α and β, which we have varied in order to study the structure of the space of solutions.

The general form of the solutions that satisfy the expansions (55) and (56) is shown in Figs. 1 and 2, where the profiles of the functions $f(r)$ and $w(r)$ are displayed, respectively, for $\alpha = \beta = 1$ for $w_\infty = \pm 1$ and the ungauged case, resulting from setting $w(r) = 1$ in the field equations.

From the energy density $\tilde{\mathcal{E}}$ [Eq. (41)], we can compute the energy of the solutions E, both for the gauged cases [$w_\infty = \pm 1$] and the ungauged one [$w(r) = 1$], as

$$E = \frac{1}{(4\pi)^2}\int \tilde{\mathcal{E}} d^4x = \frac{1}{32}\int r^3 \tilde{\mathcal{E}} dr, \tag{57}$$

where we have extracted the angular contribution and also included a $1/32$ factor to normalize the topological charge q. The last equality in Eq. (57) is valid for the spherical ansatz in Eqs. (42), (45), and (46). By construction, Eq. (57) has a lower bound given by (the absolute value of) the integral of $1/(4\pi)^2$ times Eq. (34), which, evaluated over the gauged [$w_\infty = \pm 1$] and the ungauged [$w(r) = 1$] solutions, takes the value

$$|q| \equiv \left| \frac{1}{(4\pi)^2}\int \tilde{\varrho}^{(4)} d^4x \right| = 1. \tag{58}$$

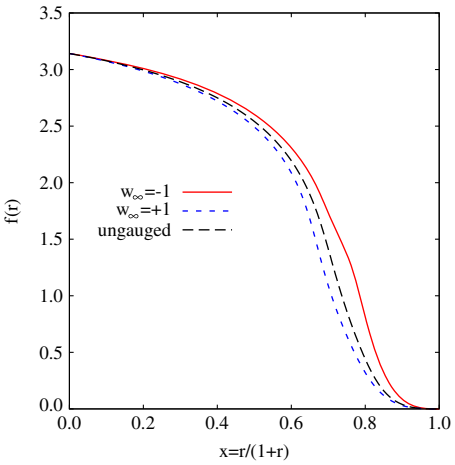


FIG. 1. The profile of the function $f(r)$ for a typical solution is shown for $\alpha = \beta = 1$, both for the gauged and the ungauged cases.

In Fig. 3, we represent the energy density $\tilde{\mathcal{E}}(r)$ as a function of the radial coordinate. Note that it presents its maximal value at the origin for all the types of solutions considered here.

The analysis of the dependence of the energy E on α and β is carried out in the subsequent figures. In Figs. 4 and 5, we fix one of the parameters and move the other one, for the gauged [$w_\infty = \pm 1$] and the ungauged [$w(r) = 1$] solutions, presenting the results in logarithmic scale. The lower bound is also displayed. From these plots, one can see that the energy of gauged $w_\infty = -1$ solutions is always larger than the corresponding energy of the gauged $w_\infty = +1$

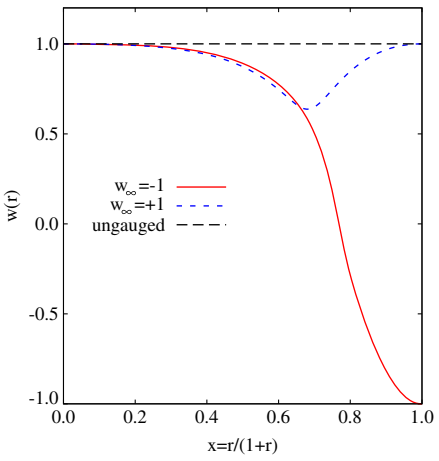


FIG. 2. The profile of the function $w(r)$ for a typical solution is shown for $\alpha = \beta = 1$, for both the gauged and the ungauged cases.

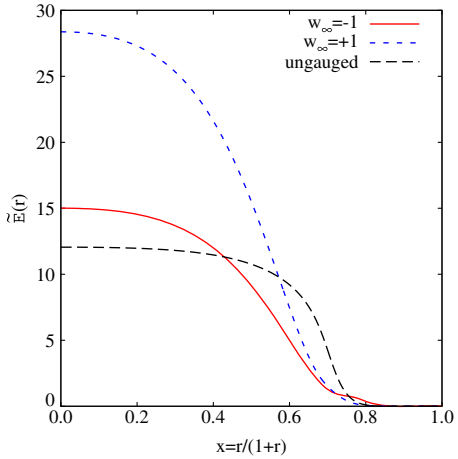


FIG. 3. Energy density $\tilde{\mathcal{E}}(r)$ for solutions with $\alpha = \beta = 1$, both for the gauged and the ungauged cases.

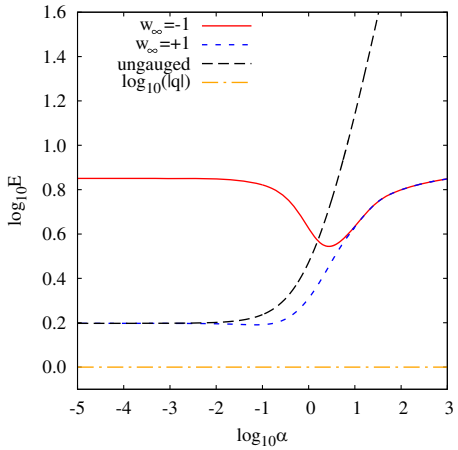


FIG. 4. Energy E versus the parameter α for fixed $\beta = 0.1$, in logarithmic scale.

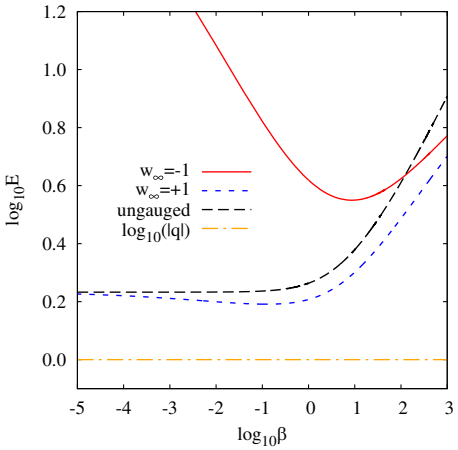


FIG. 5. Energy E versus the parameter β for fixed $\alpha = 0.1$, in logarithmic scale.

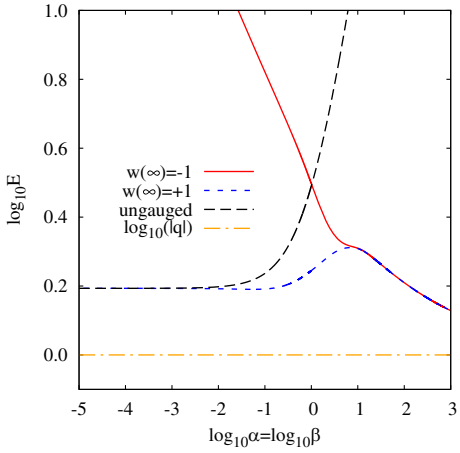


FIG. 6. Energy E versus the parameter $\alpha = \beta$.

solutions. When compared to the energy of the ungauged solutions, whereas the gauged $w_\infty = +1$ solutions always have lower energy than the ungauged ones, the gauged $w_\infty = -1$ solutions have larger energy than the ungauged ones for small values of α and/or β, but their energy gets lower than that of the ungauged solutions beyond a certain value of the parameters.

Although the analysis of the full (α, β) parameter space is computationally too costly, we can further support our previous statements by considering the $\alpha = \beta$ set of solutions. Their energy is represented as a function of $\alpha = \beta$ in Fig. 6. In this plot, one feature that is also present in Figs. 4 and 5 can be clearly seen—namely, that in the large α and/or β limit, the energies of gauged $w_\infty = -1$ and $w_\infty = +1$ solutions tend to coincide. In fact, for $\alpha = \beta$, they approach the lower bound more and more in the large $\alpha = \beta$ limit. As a final comment, we will indicate that the gauged $w_\infty = +1$ solutions show a local (not global) minimum of the energy, which is absent for the gauged $w_\infty = -1$ solutions and the ungauged ones. It is approximately located at $(\alpha, \beta) = (0.055, 0.055)$, as graphically shown in Fig. 7.

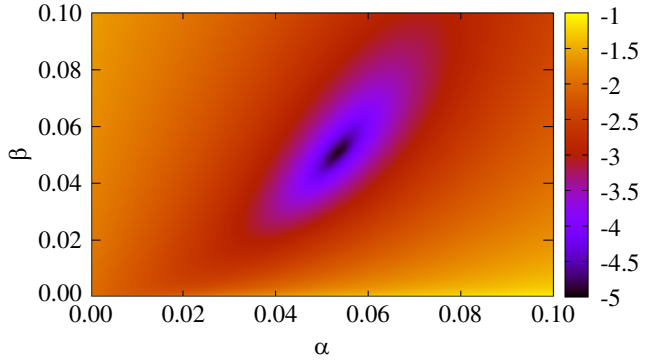


FIG. 7. Detail of the local minimum of the energy of gauged $w_\infty = +1$ solutions, where $\log_{10}(E - 1.55)$ is shown on the (α, β) plane.

V. SUMMARY AND DISCUSSION

We have studied an $SO(4)$ gauged $O(5)$ Skyrme model on $\mathbb{R}^4$ in some detail, including quantitative aspects numerically. This is a sequel to the seminal work [1] of the $SO(2)$ gauged $O(3)$ Skyrme model on $\mathbb{R}^2$, and the corresponding work [4–7] of the $SO(3)$ gauged $O(4)$ Skyrme model on $\mathbb{R}^3$. As such, it points out the path to the construction of such models for all D—namely, $SO(D)$ gauged $O(D+1)$ Skyrme models supporting solitons on $\mathbb{R}^D$. The most striking differences between the $D=2$ case [1] and the $D=3$ case [4,5], as well as here in the $D=4$ case, are that in $D=2$, solutions to the first-order equations saturating the topological lower bound exist, while in $D=3$ and 4, the corresponding "Bogomol'nyi equations" are overdetermined, and only solutions to the full second-order equations exist. Moreover, while analytic proofs for the existence in $D=2$ are given in Refs. [9–11], in $D=3$, 4, the existence of solutions to the second-order ODEs subject to radial symmetry are given numerically.

Having claimed that the $D=4$ example presented here points the way to the case of arbitrary D, it is perhaps appropriate to point out that the number of free parameters characterizing the models increases with increasing D. The $D=3$ case studied in Ref. [5] features only one parameter—say, κ—while here in $D=4$, the parameter space is described by two numbers (α,β), as formulated in Sec. II B.

There is yet another aspect of the proliferation of choice of models with increasing D. Here in $D=4$, we have chosen the energy density functional [Eq. (33)] and have eschewed the option alluded to in footnote 2, since in that case the model would not feature a quadratic Skyrme kinetic term. It is clear that such proliferation of choices will increase with increasing D.

A notable property of solutions in $D=3$ studied in Ref. [5] and those studied here in $D=4$ is that there occur two branches of solutions in each case. In $D=3$, the mass/energy E versus κ plot (E,κ) [5] features a swallow's tail [19], while here in $D=4$ no such (swallow's tail) structures are observed in the (E,α) and (E,β) profiles. In both the $D=3$ and $D=4$ cases, the two branches of solutions are characterized by the asymptotic value of the function $w_\infty \stackrel{\text{def.}}{=} \lim_{r\to\infty} w(r)$, and in both cases, *only* one of these branches is connected to the gauge decoupling limit of the Skyrmion.

In $D=3$, each of these two branches terminates at a finite value of κ—say, κ_1 and κ_2—which coexist in a certain range and are connected by a third branch that forms the swallow's tail. Only one of these branches connects with the gauge decoupled Skyrmion, and the whole (E,κ) profile lies below the corresponding profile for the ungauged Skyrmion.

In $D=4$, by contrast, the two branches, both parametrized by (α,β), are present in the whole range and do not stop anywhere in α or β. Moreover, only one of these is connected to the gauge decoupled Skyrmion, and, as expected, its energy is always smaller than that of the ungauged Skyrmion. The other branch, which does not have a gauge decoupling limit, can have energy larger than the ungauged Skyrmion in some parts of parameter space.

It would be interesting to learn what is the source of this difference in the energy profiles in $D=3$ and $D=4$. A marked difference between even and odd dimensions is the presence of a Pontryagin density, which enters the definition of the topological charge and results in the appearance of the "pion mass"-type potential via the Bogomol'nyi-like lower bounds. This is the case in both $D=2$ [1] and here in $D=4$—in the first case, there being a single branch, and here, the two branches covering the whole parameter space. In $D=3$ by contrast, in the absence of a Pontryagin density, no "pion mass"-type potential appears naturally [20]. This question can be settled by studying the $SO(5)$ gauged $O(6)$ Skyrmion on $\mathbb{R}^5$, which may be a subject of future investigation.

Finally, it is perhaps in order to point out a technical interpretation of the solutions constructed here as instantons, by reassigning the "energy" E of the Skyrmion in $4+1$ dimensions as the "action" S on $\mathbb{R}^4$. Like the BPST instanton [21], the two types of solutions here [characterized by the asymptotic values $w_\infty=\pm 1$ of the function $w(r)$] have a function $w(r)$ that decays as r^{-2}, and their actions are bounded below by the topological charge, which is the winding number in this case. Unlike the BPST instantons, which satisfy first-order equations saturating the lower bound, the solutions here do not saturate the lower bound, but in contrast to the former [21], which are localized to an arbitrary scale, these are localized to an absolute scale.

The difference between the BPST instanton [21] and the solutions here is that the former are described by (anti-)self-dual $SU_\pm(2)$ connections, while the solutions here are described by an $SO(4)$ connection, although between them, there is a curious similarity.

The curvature $F^{(\pm)}_{\mu\nu}$ of the $SU_\pm(2)$ connection

$$A^{(\pm)}_\mu = A^{ab}_\mu \sigma^{(\pm)}_{ab}, \qquad \sigma^{(\pm)}_{ab} = -\frac{1}{4}\left(\frac{1\pm\gamma_5}{2}\right)[\gamma_\mu,\gamma_\nu], \tag{59}$$

satisfying the first-order (anti-)self-duality equation

$$F^{(\pm)}_{\mu\nu} = \pm\frac{1}{2}\varepsilon_{\mu\nu\rho\sigma}F^{(\pm)}_{\rho\sigma} \tag{60}$$

yields, subject to spherical symmetry, the familiar charge-1 BPST (anti-)instanton.

The solutions to Eq. (60) happen to coincide with those to the double–self-duality equations

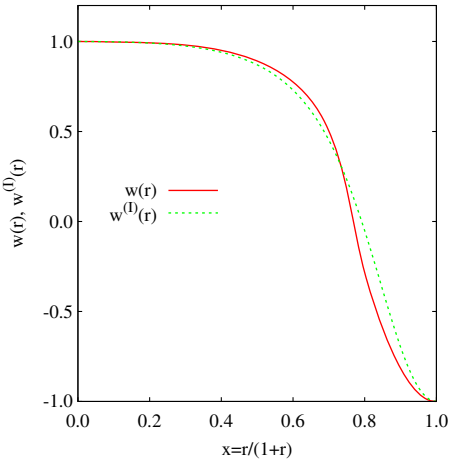


FIG. 8. Functions $w(r)$ and $w^{(I)}(r)$ for the solution with $\alpha = \beta = 1, w_\infty = -1$, and the BPST solution for $\lambda = 0.26334$.

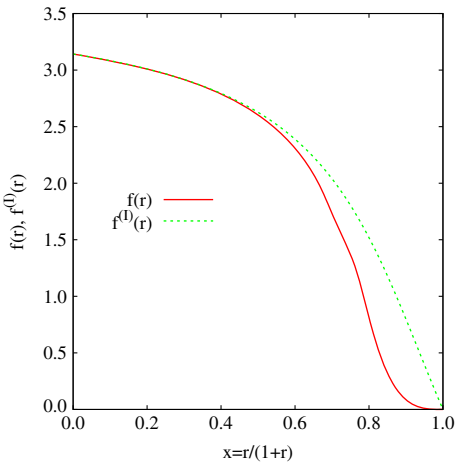


FIG. 9. Functions $f(r)$ and $f^{(I)}(r)$ for the solution with $\alpha = \beta = 1, w_\infty = -1$, and the BPST solution for $\lambda = 0.26334$.

$$F^{ab}_{\mu\nu} = \pm \frac{1}{(2!)^2} \varepsilon_{\mu\nu\rho\sigma} \epsilon^{abcd} F^{cd}_{\rho\sigma}, \tag{61}$$

which, for the radially symmetric $SO(4)$ connection [Eq. (42)], yields the same function $w(r)$ that parametrizes the BPST (anti-)instantons.

The function $w^{(I)}(r)$ solving the double–self-duality equation (61) coincides with the BPST function

$$w^{(BPST)}(r) = \frac{1 - \lambda^2 r^2}{1 + \lambda^2 r^2}, \tag{62}$$

which is also a solution to the full second-order equations of the $SO(4)$ gauge field on $\mathbf{R}^4$.

But the function $w(r)$ describing the second-order equations of the model (33) differs from $w^{(I)}(r)$, since the first-order double–self-duality equations saturating the inequalities (21), (25), and (29) are overdetermined.

We have plotted the function $w^{(I)}(r)$ in Fig. 8, and the chiral function [22]

$$f^{(I)}(r) = \pi - \arccos w^{(I)}(r) \tag{63}$$

in Fig. 9, to contrast them with the profiles of $w(r)$ and $f(r)$ that solve the second-order equations of the model (33), for the $\alpha = \beta = 1$, $w_\infty = -1$ case. For the BPST solution, λ has been chosen such that $df/dr(0) = df^{(I)}/dr(0)$ (i.e., $\lambda = 0.26334$).

Although the main behavior of the two types of solutions is similar, the main discrepancy occurs at infinity, where the presence of a potential [Eq. (23)] forces the function $f(r)$ in our solutions to decay as $1/r^3$, while for the BPST solution $f^{(I)}(r)$ decays as $1/r$.

Unfortunately, the solitons with *instanton boundary values* presented here cannot be employed to construct a *dilute gas* of instantons as in Sec. 3 of Ref. [23]. This is because the soliton employed in [23] is a *magnetic monopole* which describes a symmetry-breaking field configuration, and which allows gauging away of the order parameter (Higgs field), while the order parameter (Skyrme scalar) here cannot be gauged away, as that model does not describe a *symmetry-breaking* theory.

To enable the construction of a dilute gas of instantons on $\mathbf{R}^4$, a model of the $SO(4)$ gauged Higgs scalar ϕ^a, $a = 1, 2, 3, 4$ must be employed. But in the spherically symmetric case, the lower bounds analogous to Eqs. (29) and (31) result in *monopole asymptotic behavior*, which, subject to the requirement of finite action, excludes the presence of an F^2 curvature-squared term in the action density, leaving only an F^4 term, which decays too fast and leads to the vanishing of the dilute gas action. This obstacle can be overcome by seeking monopole-antimonopole solutions subject to biazimuthal symmetry (as, e.g., in Ref. [24]) that can describe finite-action solutions with *instanton boundary conditions*, allowing the presence of an F^2 term that on $\mathbf{R}^4$ supports a dilute gas. This is a challenge to which we plan to return.

ACKNOWLEDGMENTS

Special thanks to Eugen Radu for constant discussions during the preparation of the manuscript. We thank Yves Brihaye and Derek Harland for valuable discussions and comments on the manuscript, and Yisong Yang for earlier discussions and for bringing Refs. [9–11] to our attention. We acknowledge helpful discussions with Ernesto Canfora, Bjarke Gudnason, and Parameswaran Nair. One of us (D. H. T.) thanks Kieran Arthur for his early work on this subject. F. N.-L. gratefully acknowledges support from MICINN under Project No. PID2021-125617NB-I00 "QuasiMode."

DATA AVAILABILITY

The data that support the findings of this article are not publicly available. The data are available from the authors upon reasonable request.

[1] B. J. Schroers, Bogomolny solitons in a gauged $O(3)$ sigma model, Phys. Lett. B **356**, 291 (1995).

[2] By Skyrmion, here is meant the soliton of the $O(D+1)$ Skyrme scalar on $\mathbb{R}^D$:

$$\phi^A = (\phi^a, \phi^{D+1}); A = a, D+1; a = 1, 2, \ldots, D$$

with $|\phi^A|^2 = |\phi^a|^2 + (\phi^{D+1})^2 = 1$, which in $D = 3$ is parametrized as $U = \phi^4 \mathbb{1} + \phi^a \sigma_a$ in the original work [3] of Skyrme.

[3] T. H. R. Skyrme, Particle states of a quantized meson field, Proc. R. Soc. A **262**, 237 (1961).

[4] K. Arthur and D. H. Tchrakian, $SO(3)$ gauged soliton of an $O(4)$ sigma model on $\mathbb{R}^3$, Phys. Lett. B **378**, 187 (1996).

[5] Y. Brihaye and D. H. Tchrakian, Solitons/instantons in d-dimensional $SO(d)$ gauged $O(d+1)$ Skyrme models, Nonlinearity **11**, 891 (1998).

[6] J. Cork, Skyrmions from calorons, J. High Energy Phys. 11 (2018) 137.

[7] J. Cork, D. Harland, and T. Winyard, A model for gauged skyrmions with low binding energies, J. Phys. A **55**, 015204 (2022).

[8] J. Cork and D. Harland, Geometry of gauged skyrmions, SIGMA **19**, 071 (2023).

[9] Y. Yang, A necessary and sufficient condition for the existence of multisolitons in a self-dual gauged sigma model, Commun. Math. Phys. **181**, 485 (1996).

[10] Y. Yang, *Solitons in Field Theory and Nonlinear Analysis* (Springer, New York, 2001).

[11] J. Han and H. Huh, Existence of solutions to the self-dual equations in the Maxwell gauged $O(3)$ sigma model, J. Math. Anal. Appl. **386**, 61 (2012).

[12] D. H. Tchrakian, Gauged Skyrme analogue of Chern-Pontryagin, J. Phys. A **58**, 015401 (2025).

[13] E. B. Bogomol'nyi, Stability of classical solutions, Sov. J. Nucl. Phys. **24**, 449 (1976).

[14] F. Navarro-Lérida and D. H. Tchrakian, Vortices of $SO(2)$ gauged Skyrmions in $2+1$ dimensions, Phys. Rev. D **99**, 045007 (2019).

[15] N. M. Romão and J. M. Speight, The geometry of the space of BPS vortex-antivortex pairs, Commun. Math. Phys. **379**, 723 (2020).

[16] Alternatively, one can invoke the inequality

$$|\phi^{AB}_{\mu\nu} - \tilde{\phi}^{AB}_{\mu\nu}|^2 \geq 0,$$

in which $\tilde{\phi}^{AB}_{\mu\nu}$ is defined as

$$\tilde{\phi}^{AB}_{\mu\nu} = \frac{1}{2^2} \varepsilon_{\mu\nu\rho\sigma} \varepsilon^{ABCDE} \phi^{CD}_{\rho\sigma} \phi^E,$$

such that $\phi^{AB}_{\mu\nu} \tilde{\phi}^{AB}_{\mu\nu} = 2\varrho^{(4)}_G$. We have eschewed this option of introducing $\varrho^{(4)}_G$, since in that case, the resulting energy density does not feature a quadratic Skyrme kinetic term $|\phi^A_\mu|^2$. Also, in that case, Derrick scaling is not satisfied in the gauge decoupling limit.

[17] This is not the term $|\phi^{AB}_{\mu\nu}|^2$, which is invariant against the global $SO(5)$ rotations of the $O(5)$ model, which is given by the simpler expression

$$|\phi^{AB}_{\mu\nu}|^2 = 2 \times 3! \left(\frac{w \sin f}{r}\right)^2 \left[(f')^2 + \left(\frac{w \sin f}{r}\right)^2\right]$$

instead.

[18] U. Ascher, J. Christiansen, and R. D. Russell, A collocation solver for mixed order systems of boundary value problems, Math. Comput. **33**, 659 (1979).

[19] Y. Brihaye, B. Kleihaus, and D. H. Tchrakian, Dyon-Skyrmion lumps, J. Math. Phys. (N.Y.) **40**, 1136 (1999).

[20] Should such a potential be added *by hand*, the situation may change, but this would go beyond the minimal models implied by the Bogomol'nyi-like inequalities.

[21] A. A. Belavin, A. M. Polyakov, A. S. Schwartz, and Y. S. Tyupkin, Pseudoparticle solutions of the Yang-Mills equations, Phys. Lett. **59B**, 85 (1975).

[22] The chiral function $f^{(I)}(r)$ here parametrizes the $O(5)$ Skyrme scalar $\phi^{\bar{a}} = (\phi^a, \phi^5)$, with

$$\phi^a = \hat{x}^a \sin f^{(I)} \quad \text{and} \quad \phi^5 = \cos f^{(I)}$$

satisfying the double–self-duality equation

$$\phi^{\bar{a}\,\bar{b}}_{\mu\nu} = \pm \frac{1}{2^2} \varepsilon_{\mu\nu\rho\sigma} \varepsilon^{\bar{a}\,\bar{b}\,\bar{c}\,\bar{d}\,\bar{e}} \phi^{\bar{c}\,\bar{d}}_{\rho\sigma} \phi^{\bar{e}},$$

where $\phi^{\bar{a}\,\bar{b}}_{\mu\nu} = \partial_{[\mu} \phi^{\bar{a}} \partial_{\nu]} \phi^{\bar{b}}$.

[23] A. M. Polyakov, Quark confinement and topology of gauge groups, Nucl. Phys. **B120**, 429 (1977).

[24] E. Radu and D. H. Tchrakian, Self-dual instanton and non-self-dual instanton–anti-instanton solutions in $d = 4$ Yang-Mills theory, Phys. Lett. B **636**, 201 (2006).